Hindawi
Journal of Advanced Transportation
Volume 2019, Article ID 6126408, 10 pages
https://doi.org/10.1155/2019/6126408

Research Article

An Initial Investigation of the Effects of a Fully Automated Vehicle Fleet on Geometric Design

John Khoury,[1] **Kamar Amine**,[1] **and Rima Abi Saad**[2]

[1]*Department of Civil Engineering, Lebanese American University, PO Box #36, Byblos, Lebanon*
[2]*Department of Civil Engineering, NJIT, NJ, USA*

Correspondence should be addressed to John Khoury; john.khoury@lau.edu.lb

Received 12 February 2019; Revised 25 April 2019; Accepted 15 May 2019; Published 26 May 2019

Academic Editor: Eleonora Papadimitriou

Copyright © 2019 John Khoury et al. This is an open access article distributed under the Creative Commons Attribution License, which permits unrestricted use, distribution, and reproduction in any medium, provided the original work is properly cited.

This paper investigates the potential changes in the geometric design elements in response to a fully autonomous vehicle fleet. When autonomous vehicles completely replace conventional vehicles, the human driver will no longer be a concern. Currently, and for safety reasons, the human driver plays an inherent role in designing highway elements, which depend on the driver's perception-reaction time, driver's eye height, and other driver related parameters. This study focuses on the geometric design elements that will directly be affected by the replacement of the human driver with fully autonomous vehicles. Stopping sight distance, decision sight distance, and length of sag and crest vertical curves are geometric design elements directly affected by the projected change. Revised values for these design elements are presented and their effects are quantified using a real-life scenario. An existing roadway designed using current AASHTO standards has been redesigned with the revised values. Compared with the existing design, the proposed design shows significant economic and environmental improvements, given the elimination of the human driver.

1. Introduction

Recently, major efforts have been exerted to increase safety on roadways and reduce crashes. NHTSA's 2015 Fact Sheet highlights that human error is the main cause of 94% of motor crashes in the USA [1]. Engineers have been developing driving systems that gradually reduce and eventually eliminate the need for a human driver, thus reducing the human error associated with the most vehicle crashes [2].

In the past few years, autonomous vehicles have been gradually introduced to the highway network. Those vehicles are equipped with different levels of driver assistance systems, from basic levels of cruise-control and self-parking to fully autonomous vehicles requiring no human intervention. SAE has identified six levels of vehicle automation, ranging from Level 0 to Level 5. By eliminating the need for a human driver, the automation of vehicles is expected to reduce traffic and accident risks [3]. Given the rapid progression in vehicle automation, drivers are willing to let go [4] eventually turning the entire fleet to level 5, fully autonomous driverless vehicles. Highways will go through a transitional period serving mixed vehicle fleets composed of conventional vehicles with their human drivers and autonomous vehicles simultaneously, before reaching a 100-percent level 5 autonomous vehicle fleet. Once the entire vehicle fleet comprises fully autonomous vehicles, geometric design standards bound by human drivers' parameters/factors can be revised.

2. Background

2.1. Evolution of Autonomous Vehicles. The concept of cars with no human driver started with remotely controlled autonomous cars which emerged in the early 1920s with the release of Pontiac's "phantom auto" [5]. From then on, the concept has been under constant development. In 1939, GM released its vision of automated highways which were imagined as advanced highways that could keep the car in its lane and maintain its speed [6]. By the 1960s, visions of autonomous vehicles smart enough to sense, process, and react emerged. Yet, the ability to imitate the human driver remained a challenge [7]. In the 1980s, the USA released plans for executing a prototype of an Automated Highway System (AHS). Provisions of the AHS involved a system of in-road magnets that helped control the vehicles' movements.

Between the 1980s and the 1990s, Ernst Dickmanns tested several prototypes of autonomous vehicles that could steer themselves using sensors and intelligent software [6, 7]. From 2004 to 2007, the Defense Advanced Research Projects Agency (DARPA) conducted three challenges involving autonomous vehicle [8]. The challenges comprised teams racing a specific distance using autonomous vehicles under full autonomous mode. In 2009, Google's self-driving project was established. Driver-assisted vehicles appeared, where the driver needed to take over in complex situations. By June 2018, Google's fleet of autonomous vehicles had covered over seven million miles in autonomous mode, without any manual interference [9]. In 2015, Google released the first customized model of an autonomous vehicle, after testing the autonomous system on ordinary vehicles, such as Toyota and Lexus, to allow human driver intervention in case of emergencies [10]. The car, named "firefly," performed its first trip on public roads with a blind passenger inside, without any incidents.

Various supporting systems have been under testing and development to facilitate autonomous vehicles operations. While many systems focused on vehicle operations along uninterrupted highways [11, 12], many focused on autonomous vehicles crossing intersections to improve efficiency and safety and reduce delay [13–16]. To achieve a high degree of safety and accuracy in autonomous vehicles, several sensors and radars are used to instantly map the road ahead. One main component of current autonomous vehicles is the Light Detection and Ranging (LiDAR) sensor. LiDAR is a remote sensing method that depends on light to measure variable distances to Earth. It can process 1.33 million points per second of the surrounding environment [17]. Proceeding from the concept of LiDAR, Waymo created its own LiDAR sensor that not only detects objects or pedestrians all around the vehicle but also determines the direction pedestrians are facing. This customized sensor guarantees a more detailed view and safer operations. In 2018, the company partnered with Jaguar to build 20,000 self-driving vehicles [10]. On April 2019, Waymo launched its first live televised ride highlighting the safety and reliability of their vehicles [18]. Several automobile companies have started developing fully autonomous vehicles with their customized sensors. Companies such as Nissan, Ford, GM, and Volkswagen have already promised that autonomous vehicles will be on roads or in production between 2020 and 2022 [19–22].

2.2. Development of Highway Geometric Design Elements. Highway engineering textbooks, since the early 1900s, presented design guidelines for horizontal and vertical curves, drainage systems, pavements, lane widths, street intersections, and other aspects of highway design [23–26]. The stopping sight distance (SSD) dictates the safe distance a human driver needs to perceive, react, brake, and stop before hitting an obstacle. The SSD accounts for the perception-reaction time (PRT) of most drivers. It was first mentioned in Blanchard and Drowne's Textbook on Highway Engineering published in 1914 without assigning specific values. The first numerical reference to SSD was given in 1916 by Agg. He stated that there should always be a clearance of at least 250 feet of the view ahead, when designing rural highways [23]. In 1924, Agg increased the SSD distance from 250 to 400 feet [26]. In 1926, Brightman advised providing 500 feet of sight distance, which was adopted by AASHO two years later as a minimum requirement [27]. In 1935, Baldock defined SSD as the "distance travelled during the reaction time of the operators plus the braking distance" [25], which is still the current definition. Later that year, Wiley defined SSD as the maximum distance at which two vehicles are mutually visible. It is set by experience to be around 600 feet for both horizontal and vertical curves [26]. Another reference to SSD was given in the mid-1930s by the State of Ohio's Department of Highways [27]. It specifically referred to the sight distance on vertical curves and presented three values for minimum sight distance: 1000 feet on two-lane, 1500 feet on three-lane, and 800 feet on four-lane highways [27]. Finally, AASHTO's current model adopts a PRT of 2.5 seconds following an experiment performed by Johansson and Rumar on 321 alert drivers, in addition to other groups that were tested under different circumstances [28]. This value exceeds the 90th percentile of reaction times of all drivers [29]. Table 1 lists the historical development of the SSD model since 1914 and summarizes all the changes it went through (US units are exceptionally used in this table to maintain exact values found in the literature).

Table 1: Development of SSD model [27].

Source (Author/year)	PRT (sec)	Sight distance (feet)
Agg, 1916		At least 250
Agg, 1924		400
Michigan, 1926		500
Oregon, 1935	0.5	1,500 @ 80 mph
Wiley, 1935		600
Ohio, 1937		1,000 (two lanes) 800 (four lanes)
Conner, 1937		500 (four lanes)
HRB, 1937	3	
Bateman, 1939		800 (Horiz C)
Agg, 1940	<1	
AASHO, 1940	3 @ 30 mph 2 @ 70 mph	200 @ 30 mph 600 @ 70 mph
AASHO, 1954	2.5	
AASHO, 1965	2.5	
AASHTO, 1970	2.5	
AASHTO, 1984	2.5	200 @ 30 mph 850 @ 70 mph
NCHRP, 1984	2.5	

Fambro and Fitzpatrick [30] reassessed the SSD model, citing no evidence that longer SSD results in fewer accidents. They suggested a new and simpler model based on driver performance. In 1989, Neuman [31] suggested that functional highway classifications be the basis for determining SSD design policies and values. The study identifies five highway system classifications: low-volume road, two-lane primary rural highway, multilane urban arterial, rural freeway, and urban freeway. Compared to the current AASHTO model,

the latter model shows lower SSD values on low-volume roads and higher values on rural and urban freeways. In 2017, Wood and Donnell [32] revised the SSD model in a different context to improve accuracy and safety. Their goal was to improve the reliability of the SSD model by accounting for lighted versus unlighted-nighttime conditions. Glennon [33] criticized AASHTO's SSD model and other sight distance models for being too conservative. Harwood et al. [34] reassessed the parameters of the SSD model and evaluated its effect on horizontal and vertical alignments if trucks were used as design vehicles instead of passenger cars. They suggested that trucks with conventional braking systems require longer SSD than 1984 AASHTO's recommendation.

The mentioned studies updated the current parameters of the SSD model to improve accuracy and safety of the model for human drivers. Washburn's online course [35] briefly discussed autonomous vehicles and their potential effects on traffic flow and geometric design. The course concluded that since autonomous vehicles are equipped with LiDAR and other vision sensors, the vehicles would recognize obstacles better that humans do, but their line of sight could still be obstructed at horizontal curves. As the pertinent literature mainly focuses on the effect of automated vehicles on traffic flow and highway capacity, a limited number of studies investigated the effect of vehicles on highway geometric design elements.

3. Methodology

The SSD and the DSD models are directly based on the driver's PRT, in addition to the braking distance. They are key elements in designing vertical and horizontal alignments and locating highway signs. In this section, these models will be evaluated using revised parameters to capture the effect of autonomous vehicles on highway design elements. The driver's eye height and the degree of illumination of the headlight beam are also key elements in designing crest and sag vertical curves, respectively. The latter concepts will also be reassessed. The review of the mentioned highway geometric design parameters assumes that only fully autonomous vehicles are using newly designed and constructed roads, rather than current roads being redesigned to be shared by vehicles with different levels of autonomy. Farah et al. [36] concluded that the current research trends focus on the impact of automated and connected vehicles on digital infrastructure rather than physical infrastructure. Other studies inferred that cross-sectional width standards such as lane width and shoulder requirements are expected to decrease without providing a quantitative assessment to support the conclusion [37], and very little is mentioned relative to the impacts on vertical alignments. McDonald highlighted the highway geometric design elements that may be influenced by an automated vehicle only fleet and specifically pointed out the sensitivity of the SSD to perception reaction time [38]. Garcia et al. [39] analyzed the effect of the design of crest vertical curves, based on current standards, on the driving experience of semiautonomous vehicles. The article quantified the rate of curvature and grade change, which allow the vehicle driving system to transfer between manual and automatic transmission. Their study relied on the widely available technology: radars and video cameras. In this paper, we reevaluate and test current geometric design models assuming full autonomous fleet. The elimination of the driver will have direct effects on highway design criteria, such as the SSD and DSD models.

3.1. SSD Model. The current SSD equation is a sum of two distances: the distance traveled during PRT and the distance traveled during braking [29]. The distance traveled during braking will mostly depend on vehicle properties, in addition to driver braking preferences and behavior. However, in this research, the dynamic properties of autonomous vehicles and conventional vehicles are assumed to be identical, and the surface road conditions and grade are assumed to remain the same; thus, the braking distance is assumed to remain the same. The distance traveled during PRT is the product of the design speed of the vehicle and the PRT of the driver (a constant value of 2.5 seconds [29]).

3.1.1. Current Model Equations for Human Driven Vehicles. The current SSD model equations are retrieved from AASHTO's Policy on Geometric Design of Highways and Streets (referred to as the "*Green Book*" hereafter), 6th edition, Chapter 3, pages 4-5.

(1) SSD on Level Roads (In Metric Units)

$$SSD = 0.278Vt + 0.039\left(\frac{V^2}{a}\right) \tag{1}$$

(2) SSD on Grade (In Metric Units)

$$SSD = 0.278Vt + \frac{V^2}{254\,[(a/9.81) \pm G]} \tag{2}$$

where

V (km/h) is the design speed.

t (2.5 seconds) is the driver's PRT.

a (3.4 m/s^2) is the deceleration rate.

G (decimal) is the roadway grade.

3.1.2. Proposed Model Values for an Autonomous Vehicle Fleet. After extensive machine simulations and computational efforts, the reaction time of an autonomous vehicle from the moment an obstacle is recognized to the moment the brakes are applied was found to be in the order of 0.5 seconds [40]. Assuming a full autonomous vehicle fleet, a conservative braking reaction time of exactly 0.5 seconds is chosen to replace AASHTO's driver's reaction time of 2.5 seconds. Equations (1) and (2) are maintained in the proposed SSD model equations, while changing the reaction time from 2.5 seconds to 0.5 seconds. The resulting SSD values for different design speeds and selected vertical grades are presented in Figure 1.

3.2. DSD Model. The main purpose behind the DSD is to provide the driver enough distance in complex situations

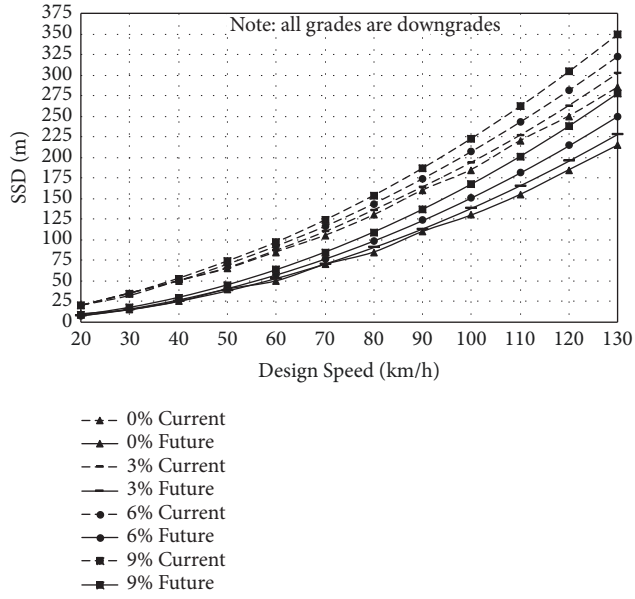

Figure 1: SSD values for current and future design standards for selected vertical grades.

to recognize a potential danger in a cluttered environment ahead, identify the threat behind it, and take the suitable decision [41]. This decision may involve bringing the vehicle to a complete stop, changing lanes, or decreasing speed. The model classifies five avoidance maneuvers with different maneuver times. Avoidance maneuvers A and B provide the stopping decision time on rural roads and urban roads, respectively. Avoidance maneuvers C, D, and E provide distance for speed, path, or direction change on rural, suburban, and urban roads, respectively. Longer maneuver times indicate more complex situations.

3.2.1. Current Model Equations for Human Driven Vehicles. The current DSD model equations are retrieved from AASHTO's *Green Book*, 6th edition, Chapter 3, pages 7 and 8.

(1) Avoidance Maneuvers A and B (In Metric Units)

$$DSD = 0.278Vt + 0.039\left(\frac{V^2}{a}\right) \quad (3)$$

(2) Avoidance Maneuvers C, D, and E (In Metric Units)

$$DSD = 0.278Vt \quad (4)$$

where

t (seconds) is the premaneuver time (other variables are already defined).

Chapter 3, Page 7 of the *Green Book* lists the premaneuver time for avoidance maneuver A, "stop on rural road," to be 3 seconds and for avoidance maneuver B, "stop on urban road," to be 9.1 seconds. For avoidance maneuver C, "speed/path/direction change on rural road," the total premaneuver time and maneuver time is listed to be between 10.2 and 11.2 seconds. For avoidance maneuver D, "speed/path/direction change on suburban road," the total premaneuver time and maneuver time is listed to be between 12.1 and 12.9 seconds. Finally, for avoidance maneuver E, "speed/path/direction change on urban road," the total premaneuver time and maneuver time is listed to be between 14 and 14.5 seconds. AASHTO's *Green Book* specifies that 3.5 to 4.5 seconds of the times, shown for avoidance maneuvers C, D, and E, comprise the maneuver times, while the remaining portion is the premaneuver time [29].

3.2.2. Proposed Model Values for an Autonomous Vehicle Fleet. Autonomous vehicles, heavily equipped with sensors and smart processors, will not need longer maneuver times for more complex driving situations, as human drivers do. Instead of customized reaction times for each avoidance maneuver type of the DSD model, a simple braking reaction time of 0.5 seconds remains applicable for avoidance maneuvers A and B. For the latter two maneuvers, the DSD model becomes the SSD model, given identical reaction times, and the values are shown in Table 2. The resulting DSD values for maneuvers C, D, and E are not presented herein and will be discussed in future work, since the listed times include the maneuver times in addition to the premaneuver times.

3.3. Length of Crest Vertical Curve

3.3.1. Current Model Equations for Human Driven Vehicles. The current model equations are retrieved from AASHTO's *Green Book*, 6th edition, Chapter 3, page 151, as follows:

(1) When Sight Distance Is Less Than Length of Curve (S<L)

$$L_{crest} = \frac{AS^2}{100\left(\sqrt{2h_1} + \sqrt{2h_2}\right)^2} \quad (5)$$

Table 2: Comparing DSD and K Values at different design speeds, current values retrieved from *Green Book* [29].

	DSD (m)			Sag curve		Crest curve	
	Current		Proposed	Rate of vertical curvature			
Design speed (km/h)	A	B	*A or B*	$K_{Current}$	$K_{Proposed}$	$K_{Current}$	$K_{Proposed}$
20	n/a	n/a	10	3	1	1	1
30	n/a	n/a	15	6	1	2	1
40	n/a	n/a	25	9	1	4	1
50	70	155	40	13	1	7	2
60	95	195	50	18	1	11	3
70	115	325	70	23	2	17	6
80	140	280	85	30	2	26	9
90	170	325	110	38	3	39	14
100	200	370	130	45	3	52	20
110	235	420	155	55	4	74	28
120	265	470	185	63	4	95	40
130	305	525	215	73	5	124	54

(2) When Sight Distance Is Greater Than Length of Curve (S>L)

$$L_{crest} = 2S - \frac{200\left(\sqrt{h_1} + \sqrt{h_2}\right)^2}{A} \quad (6)$$

where

S (m) is the sight distance.

h_1 (1.08 m) is the height of eye above the roadway surface.

h_2 (0.6 m) is the height of object above roadway surface.

A (percent) is the algebraic difference in grade.

3.3.2. Proposed Model Values for an Autonomous Vehicle Fleet. For autonomous vehicles, the eye of the vehicle is the LiDAR sensor, in addition to several other sensors, constantly scanning its surrounding. The findings of Garcia et al. [39] highlight the fact that the location of devices embedded in autonomous vehicles is an important variable in determining the available sight distance. In this regard, the higher the devices, the larger the available sight distance. The Waymo LiDAR can see objects in the size of a soccer ball as far as three football fields away in every direction. Based on that, the eye height used in computing the length of crest vertical curves in this study is replaced by height of the LiDAR sensor mounted on top of the car. The height of the LiDAR is measured from the roadway surface to the center of the lens.

The Google self-driving project started their experiments of autonomous vehicles and LiDAR testing on a Toyota Prius and a Lexus RX450h [9]. These vehicles have heights of 1.470 m and 1.685 m. After Waymo took over the project, the company manufactured its own customized car with a body like that of SMART cars. The height of the Waymo self-driving vehicle is considered equal to that of a SMART car, which is 1.555 m. In addition to the car height, the height of the LiDAR is 0.284 m [17]. We discuss two common values for h_1. Using the Lexus SUV as the reference vehicle, h_1 is the summation of the height of car roof, 1.685 m, height of LiDAR, 0.284 m, and height of LiDAR support, 0.3 m, resulting in h_1 of 2.27 m. Using Waymo Car as the reference vehicle, h_1 becomes the summation of the height of car roof, 1.555m, and height of LiDAR, 0.284 m; no support is used, resulting in h_1 of 1.84 m.

Note that as h_1 decreases, L_{crest} increases. Based on the autonomous vehicles discussed in Section 2, future autonomous passenger vehicles are assumed to have larger heights than SMART cars. Autonomous SUVs, trucks, and buses will have larger heights as well. Since vehicles with larger heights require shorter crest vertical curves, the authors assume a minimum conservative h_1 of 1.7 m. Equations (5) and (6) are maintained for length of crest vertical curves, with the height of LiDAR above roadway surface, 1.7 m, replacing the height of driver's eye of 1.08 m. In addition, the "S" value is replaced by the sight distance of an autonomous vehicle rather than the sight distance of a human driver, whether this distance is SSD or passing sight distance (PSD, which will be discussed in future work). The resulting crest vertical rate of curvature (K values) for different design speeds is presented in Table 2. AASHTO defines "K" as the horizontal curve length needed to affect 1% change in slope ($L = K.A$).

3.4. Length of Sag Vertical Curve

3.4.1. Current Model Equations for Human Driven Vehicles. The current model equations are retrieved from AASHTO's *Green Book*, 6th edition, Chapter 3, page 158, as follows:

(1) When Sight Distance Is Less Than Length of Curve (S<L)

$$L_{sag} = \frac{AS^2}{\left(200\left(H + S\tan\beta\right)\right.} \quad (7)$$

(2) When Sight Distance Is Greater Than Length of Curve (S>L)

$$L_{sag} = 2S - \frac{200\left(H + S\tan\beta\right)}{A} \quad (8)$$

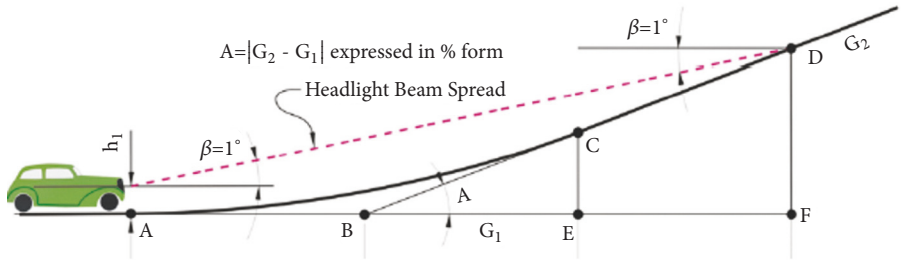

Figure 2: Inclined angle of headlight beam while being on a sag vertical curve [38].

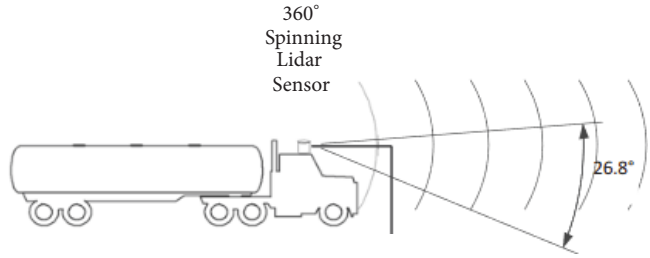

Figure 3: Vertical field of view of LiDAR sensor [17].

where

S (m) is the light beam distance taken to be equal to the SSD.

H (0.6 m) is the height of headlight above roadway surface.

β (1 degree) is inclined angle of headlight beam, shown in Figure 2.

3.4.2. Proposed Model Values for an Autonomous Vehicle Fleet. One of AASHTO's standards focuses on nighttime operations for the design of a sag vertical curve. Visibility at night depends on both, the vehicle's headlight height and the inclined angle of the headlight beam. In conventional vehicles, these are main parameters used in calculating the length of sag vertical curves. For autonomous vehicles, the LiDAR operates similarly during night or day conditions [42]. In (7) and (8), the height of the headlight is replaced by the height of the sensor above the roadway, calculated to be 1.7 meters. Similarly, the inclined angle of the headlight beam is replaced by the inclination of the vertical field of view of the LiDAR, measured from the horizontal axis of the vehicle. The field of view, according to LiDAR's manufacturer, is 26.8 degrees. A schematic of the field of view of LiDAR is shown in Figure 3 which is retrieved from the LiDAR user's manual [17]. We note that this value represents a 100th percentile value of the LiDARs because the technology is not vehicle dependent, assuming that all LiDARs will share identical properties regardless of the manufacturer. The authors found no reference in the literature discussing the inclination of the LiDAR's field of view from the vehicle's horizontal axis; thus, a 13.4-degree angle is assumed, which is half the total angle of view.

3.5. Model Applications. Using the models for each of the SSD, DSD, and length of sag and crest vertical curves, computations were performed to compare the current model values to the proposed values. The results are shown in Figure 1 and Table 2. SSD differs with the design speed as well as the grade. Under all circumstances, the proposed model yields smaller SSD requirements, as shown in Figure 1. The proposed SSD values that will replace the DSD values of the current model also yield smaller requirements for avoidance maneuvers A and B. Table 2 also displays the rate of vertical curvature, K, calculated by dividing (5) and (7) by the algebraic difference of the grades. It also varies with the design speed. Using the proposed model equations for length of crest vertical curve, K values for crest curves are smaller. K values for sag vertical curves are also smaller. The benefits of reducing the vertical curve lengths are assessed in Section 5. Besides the models affected directly by the PRT, the horizontal sightline offset (HSO) model is indirectly affected by the new PRT, through the SSD value which is incorporated in the HSO equation. This paper focuses on the models directly affected by the anticipated shift towards a fully autonomous vehicle fleet.

4. Sensitivity Analysis

4.1. SSD versus PRT. Noting that the proposed value of PRT, t = 0.5 seconds, is a conservative value, this section evaluates the effect of choosing a higher or a lower value. Figure 4 shows the variation of SSD with respect to design speed, at different values of PRT versus the current SSD model. The variation of SSD between two consecutive increments of reaction time, the latter chosen to be 0.25 seconds, is at most

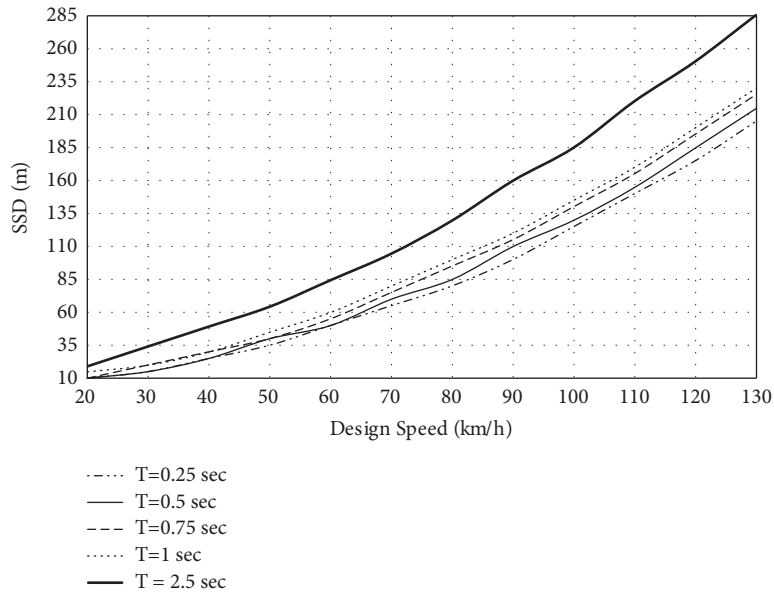

Figure 4: Variation of SSD for different PRTs.

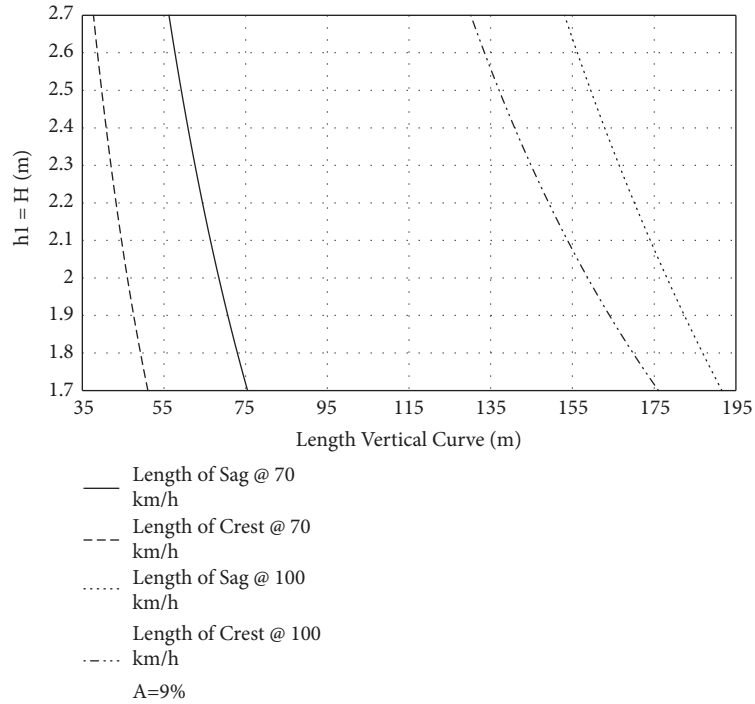

Figure 5: Variation of vertical curve length at different values of h1 and H.

10 meters. Note that the SSD values shown in Figure 4 are design values, rounded up after calculation.

4.2. Eye Height versus Length of Vertical Curve. The values of h_1 in (5), and (6), (7), and (8), chosen to be 1.7 m, are conservative values. The effect of altering the values of h_1 and H is discussed below. At two specific design speeds, 70 and 100-km/h, and an algebraic grade difference of 9%, chosen for illustration, Figure 5 shows that shorter lengths are required for increased h_1 and H values.

5. Application

To test the effects of the future proposed models on real-life designs, a roadway designed according to the current AASHTO standards is redesigned using the proposed models. The following example is the redesign of an existing road.

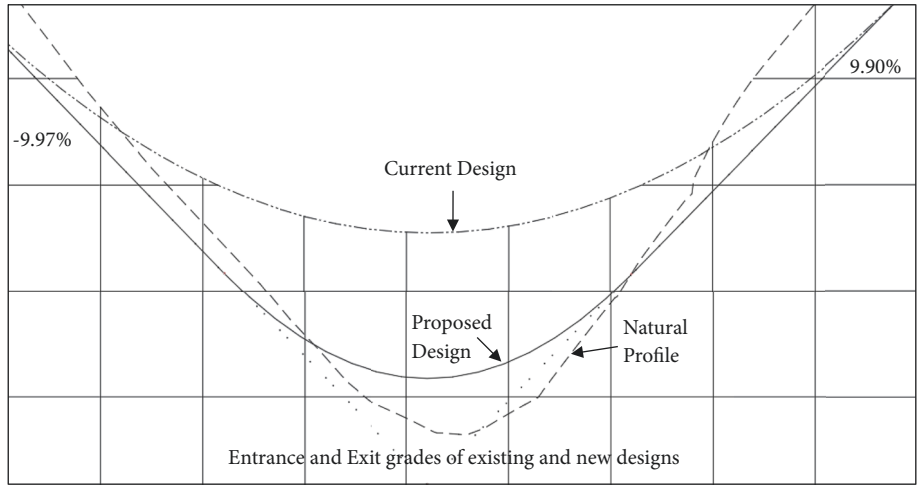

Figure 6: AutoCAD schematic of sag vertical curve #4 of Table 3: current, proposed, and natural profiles.

Table 3: Comparing lengths of vertical curves of current and proposed designs.

			Current standards design		Proposed standards design	
	Type	A (%)	K (m/%)	Length of curve (m)	K (m/%)	Length of curve (m)
Crest vertical curves						
Curve 1	Crest	4.1	23.1	95.1	5.8	24
Curve 2	Crest	9.8	23.4	228.3	2.5	24
Curve 3	Crest	8.7	23.3	203.8	2.7	24
Curve 4	Crest	7.3	23.0	167.9	3.3	24
Sag vertical curves						
Curve 1	Sag	3.4	17.0	57.1	7.1	24
Curve 2	Sag	7.4	*10.3*	76.6	4.0	30
Curve 3	Sag	6.4	13.3	85.0	4.1	26
Curve 4	Sag	19.9	9.6	191.2	4.0	80

The road has already been designed according to current standards and will be redesigned according to proposed standards to evaluate the potential effects of the suggested modifications. The design is of a local rural mountainous road in Hasbaya, Lebanon. Horizontal and vertical alignments were initially designed using AASHTO 2011 roadway design standards. The undivided roadway consists of two lanes, one in each direction. Each lane is 3.6 meters with a 1.4-meter shoulder. The design speed is 40-km/h and the roadway length is 1,781 meters. With the natural mountainous topography, the new design will test the proposed models of crest and sag vertical curves discussed in Sections 3.3.2 and 3.4.2. Since both these models include SSD as a parameter, the SSD model will be indirectly tested as well.

The initial design was performed using AutoCAD Civil3D, which allows the engineer to select the preferred design criteria files. In the proposed models, the design criteria files are updated to replace the rate of vertical curvature of the AASHTO model by that of the proposed model summarized in Table 2. To capture the effects of the reduced PRT (i.e., SSD), the grade change of every curve and the horizontal alignment are maintained unchanged in the proposed design as shown in Figure 6. The change in grade of the existing design and that of the proposed design are maintained equal, allowing for the objective comparison of the PRT effects.

5.1. Results. To compare the differences between both designs, the lengths of vertical curves are extracted and shown in Table 3. Note that sometimes the minimum K values presented in Table 2 yield smaller lengths of curves than the ones presented in Table 3, under proposed standards. That is due to other minimum requirements set by AASHTO for passenger's comfort. AASHTO recommends a minimum length of vertical curve of 0.6 multiplied by the design speed for crest curves [29] and the maximum between 0.6V and $(AV^2/395)$ for sag vertical curves, the latter constraint to ensure driver's comfort. This minimum value was used whenever the length resulting from minimum K values was smaller.

5.2. Discussion. The decrease in lengths of vertical curves shown in Table 3 has environmental and economic effects. The amount of cut and fill required to execute planned

roadways decreases when using the future standards. Generated by AutoCAD Civil3D, the required cut volume for the design under current AASHTO standards is 144,970 m^3, whereas that of the future standards is 133,854 m^3. The future standards require less cut volume by 7.67%. The required fill volume for the current design is 8,113 m^3, whereas that using the proposed standards is 4,282 m^3, resulting in a decrease of 47.22%. Figure 6 compares a sag vertical curve profile using the current design standards to the proposed design standards and also shows the natural ground profile.

The sag vertical curve in Figure 6 represents curve 4 of Table 3. Noting that the entrance and exit grades remain unchanged for both designs, the difference between the designs is clearly visible, with the proposed design requiring much less fill.

Economically, an activity with a smaller volume to cut and fill is accomplished faster and cheaper given the same productivity rate. Also, if the fill material differs from the cut material, that is, the fill material is to be purchased, a smaller volume will cost less. The future models for SSD and for lengths of sag and crest vertical curves tested in this application proved to be applicable and effective. The decrease in volumes to be cut will result in a reduced environmental footprint upon the execution of the design. That and the decrease in volumes to be filled will cost less in terms of hours required to complete the work and material required for filling.

6. Discussion and Conclusion

Highway geometric design elements are under constant research and development. The models involving a direct relationship with human factors underwent several updates to enhance their accuracy and increase roadway safety. This study evaluates the effect of having a fully autonomous vehicle fleet on highway geometric design elements. The effect of complete elimination of the human driver is investigated and design standards are reassessed resulting in proposed models that will replace the current models for the following design elements: SSD, DSD, length of crest vertical curve, and length of sag vertical curve. We note that this research does not evaluate highway geometric design standards based on the coexistence of fully autonomous vehicles and nonautonomous vehicles. The futuristic approach assumes that fully autonomous vehicles will govern the roads in the future and when they do, highway design should be reassessed.

Once fully autonomous vehicles represent 100% of the traffic fleet, the suggested changes result in cheaper road designs with a reduced environmental footprint. To quantify the effect of the updated models, a roadway previously designed according to current standards was redesigned according to the proposed future standards. The results validated the economic and environmental benefits of the proposed models through the reduced cut and fill volumes of the new design and the flexibility to use shorter vertical curves. Noting that the currently existing infrastructure provides higher capacity for a fully autonomous vehicles fleet, this research applies to prospective roads that shall be constructed in the future having a fully automated vehicle as the design vehicle.

This study represents a step forward towards the future of transportation and accounts for the presence of fully autonomous vehicles and their effect on several highway geometric design elements in a simple scenario. There are more aspects that need to be investigated and accounted for in later studies. Future work shall focus not only on the direct but also on the indirect effects of shifting towards an autonomous vehicle fleet. The reduction in the DSD models for avoidance maneuvers C, D, and E will be investigated in detail. This significant reduction in DSD will have direct impacts on current traffic design concepts and on highway signage concepts. This paper only discussed the PRT portion of the SSD model. In current practice, the SSD used in both crest and sag vertical curves equations is based on 0% grade, which differs from reality and should be accurately calculated in an autonomous vehicle environment. The current braking distance of the SSD model will also be affected and will be analyzed in more detail. Compared to human drivers, autonomous vehicles can apply the brakes harder/faster and more evenly, while better utilizing the antilock braking systems. Moreover, regarding SSD provision in autonomous vehicle environment, there are other factors besides PRT as well as the vertical location of the LiDAR that greatly affect the final SSD value. While this study takes those two parameters into consideration for a preliminary investigation, other factors should be investigated in future work.

Data Availability

The data used to support the findings of this study are available from the corresponding author upon request.

Conflicts of Interest

The authors declare that they have no conflicts of interest.

Acknowledgments

This research is funded by the Lebanese American University and the National Council for Scientific Research (Grant # 859).

References

[1] N. A. Stanton and M. S. Young, "Vehicle automation and driving performance," *Ergonomics*, vol. 41, no. 7, pp. 1014–1028, 1998.

[2] National Highway and Transportation Safety Administration (NHTSA), "Traffic safety facts. Critical reasons for crashes investigated in the national motor vehicle crash causation survey," 2015.

[3] S. Lam, J. Taghia, and J. Katupitiya, "Evaluation of a transportation system employing autonomous vehicles," *Journal of Advanced Transportation*, vol. 50, no. 8, pp. 2266–2287, 2016.

[4] R. A. Daziano, M. Sarrias, and B. Leard, "Are consumers willing to pay to let cars drive for them? Analyzing response to

autonomous vehicles," *Transportation Research Part C: Emerging Technologies*, vol. 78, pp. 150–164, 2017.

[5] A. Lafrance, "Your grandmother's driverless car," The Atlantic, 2016, https://www.theatlantic.com/technology/archive/2016/06/beep-beep/489029/.

[6] M. Weber, "Where to? a history of autonomous vehicles," Computer History Museum, 2014, http://www.computerhistory.org/atchm/where-to-a-history-of-autonomous-vehicles/.

[7] H. Lipson and M. Kurman, *Driverless Intelligent Cars and the Road Ahead*, The MIT Press, Massachusetts, Mass, USA, 2016.

[8] Defense Advanced Research Projects Agency, "Prize challenges," https://www.darpa.mil/work-with-us/public/prizes.

[9] "On the road," Waymo, https://waymo.com.

[10] "Journey," Waymo, https://waymo.com.

[11] A. Talebpour and H. S. Mahmassani, "Influence of connected and autonomous vehicles on traffic flow stability and throughput," *Transportation Research Part C: Emerging Technologies*, vol. 71, pp. 143–163, 2016.

[12] C. Letter and L. Elefteriadou, "Efficient control of fully automated connected vehicles at freeway merge segments," *Transportation Research Part C: Emerging Technologies*, vol. 80, pp. 190–205, 2017.

[13] S. I. Guler, M. Menendez, and L. Meier, "Using connected vehicle technology to improve the efficiency of intersections," *Transportation Research Part C: Emerging Technologies*, vol. 46, pp. 121–131, 2014.

[14] J. Rios-Torres and A. A. Malikopoulos, "A survey on the coordination of connected and automated vehicles at intersections and merging at highway on-ramps," *IEEE Transactions on Intelligent Transportation Systems*, vol. 18, no. 5, pp. 1066–1077, 2017.

[15] J. Khoury and J. Khoury, "Passive, decentralized, and fully autonomous intersection access control," in *Proceedings of the 2014 IEEE 17th International Conference on Intelligent Transportation Systems (ITSC)*, pp. 3028–3033, Qingdao, China, October 2014.

[16] J. Khoury, J. Khoury, G. Zouein, and J. Arnaout, "A practical decentralized access protocol for autonomous vehicles at isolated under-saturated intersections," *Journal of Intelligent Transportation Systems: Technology, Planning, and Operations*, pp. 1–14, 2019.

[17] HDL-64E S3, "User's manual and programming guide: high definition LiDAR sensor, velodyne LiDAR," 2017.

[18] H. Fernandez, "Waymo's self-driving car takes its first live televised ride-along with FBN," Fox business, 2019, http://www.foxbusiness.com/technology/waymos-self-driving-car-takes-its-first-live-televised-ride-along-with-fbn.

[19] "Nissan tests fully autonomous prototype technology on streets of Tokyo," Nissan Motor Corporation, Global Newsroom, 2017, https://newsroom.nissan-global.com/releases/release-1fc537356ae3aaf048d0201b77013bf9-171026-01-e?query=ProPILOT.

[20] "Where the VW I.D. VIZZION goes, you don't need a steering wheel," Volkswagen, Newsroom, 2018, http://newsroom.vw.com/vehicles/where-vws-i-d-vizzion-goes-you-dont-need-a-steering-wheel/.

[21] "Looking further," Ford, Innovation, https://corporate.ford.com/innovation/autonomous-2021.html.

[22] "GM takes next step toward future with self-driving vehicle manufacturing in Michigan," General Motors, 2018, https://www.gm.com/mol/m-2018-mar-0315-orion.html.

[23] A. H. Blanchard and H. B. Drowne, *Text-Book on Highway Engineering*, John Wiley & Sons, Inc, New York, NY, USA, 1914.

[24] T. R. Agg, *The Construction of Roads and Pavements*, McGraw-Hill Book Company, Inc., New York, NY, USA, 1916.

[25] R. H. Baldock, "Highway design for speeds up to 100 miles per hour," *Engineering-News Record*, pp. 732–734, 1935.

[26] C. C. Wiley, *Principles of Highway Engineering*, McGraw-Hill Book Company, Inc, 1935.

[27] J. W. Hall and D. S. Turner, "Stopping sight distance. Can we see where we now stand?" *Transportation Research Board: Journal of the Transportation Research Board*, no. 1208, pp. 4–13, 1989.

[28] G. Johansson and K. Rumar, "Drivers' brake reaction times," *Human Factors: The Journal of the Human Factors and Ergonomics Society*, vol. 13, no. 1, pp. 23–27, 1971.

[29] *A Policy on Geometric Design of Highways and Streets*, AASHTO, Washington, DC, USA, 6th edition, 2011.

[30] D. B. Fambro, K. Fitzpatrick, and R. J. Koppa, "New stopping sight distance model for use in highway geometric design," *Transportation Research Circular, Transportation Research Board, National Research Council*, vol. 1701, pp. 1–8, 1997, Washington, DC, USA.

[31] T. R. Neuman, "New approach to design for stopping sight distance," *Transportation Research Board: Journal of the Transportation Research Board*, no. 1208, pp. 14–22, 1989.

[32] J. S. Wood and E. T. Donnell, "Stopping sight distance and available sight distance: new model and reliability analysis comparison," *Transportation Research Record*, vol. 2638, no. 1, pp. 1–9, 2017.

[33] J. Glennon, "Highway sight distance design issues: an overview," *Transportation Research Record*, vol. 1208, pp. 1–3, 1989.

[34] D. W. Harwood, W. D. Glauz, and J. M. Mason Jr., "Stopping sight distance design for large trucks," *Transportation Research Record: Journal of the Transportation Research Board*, no. 1208, pp. 36–46, 1989.

[35] S. S. Washburn and L. D. Washburn, *Future Highways – Automated Vehicles*, SunCam, 2018.

[36] H. Farah, S. M. Erkens, T. Alkim, and B. van Arem, "Infrastructure for automated and connected driving: state of the art and future research directions," in *Road Vehicle Automation*, Lecture Notes in Mobility, pp. 187–197, Springer International Publishing, Cham, Swizerland, 2018.

[37] E. C. Tonias and C. N. Tonias, "Vertical parabolic curves," in *Geometric Procedures for Civil Engineers*, pp. 331–337, Springer, Cham, Swizerland, 2016.

[38] D. R. McDonald, "How might connected vehicles and autonomous vehicles influence 34 geometric design?" in *Proceedings of the Transportation Research Board 97th Annual Meeting*, vol. 35, pp. 2118–21630, 2018.

[39] A. Garcia, D. Llopis-Castello, and F. Camacho-Torregrosa, "Influence of the design of crest vertical curves on automated driving experience," in *Proceedings of the Transportation Research Board 98th Annual Meeting*, 2019.

[40] C. Urmson, "Driving beyond stopping distance constraints," in *Proceedings of the 2006 IEEE/RSJ International Conference on Intelligent Robots and Systems*, pp. 1189–1194, Beijing, China, October 2006.

[41] H. W. McGee, "Decision sight distance for highway design and traffic control requirements (abridgement)," *Transportation Research Board: Journal of the Transportation Research Board*, vol. 736, pp. 11–13, 1978.

[42] Waymo Team, "Introducing Waymo's suite of custom-built, self-driving hardware," Medium, https://medium.com/waymo/introducing-waymos-suite-of-custom-built-self-driving-hardware-c47d1714563urmson.

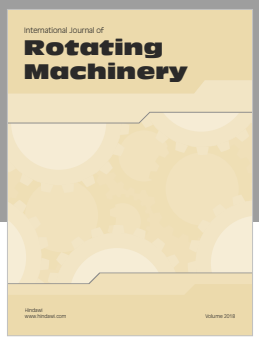

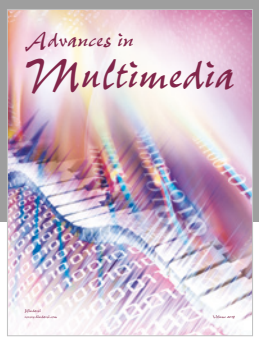

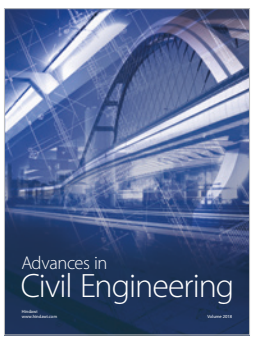

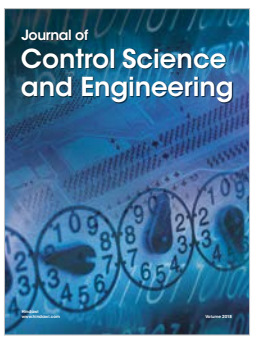

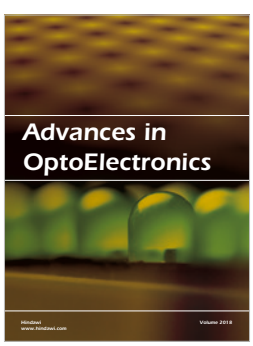

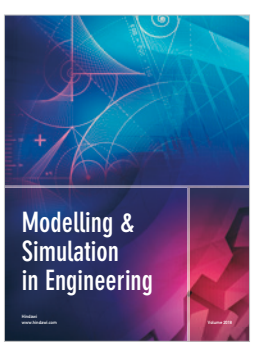

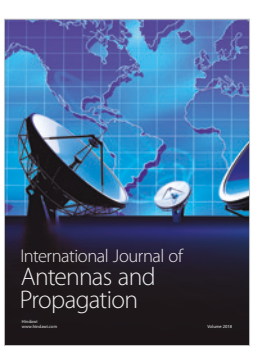

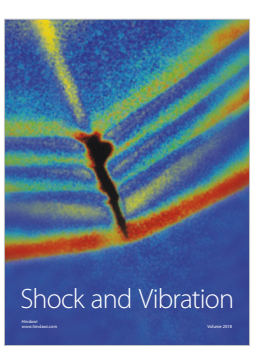

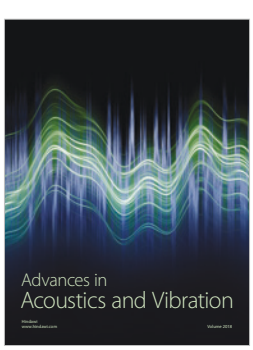

Hindawi

Submit your manuscripts at
www.hindawi.com